
Connectivity-driven Communication in Multi-agent Reinforcement Learning through Diffusion Processes on Graphs

Emanuele Pesce¹ Giovanni Montana¹

Abstract

We discuss the problem of learning collaborative behaviour in multi-agent systems using deep reinforcement learning (DRL). A connectivity-driven communication (CDC) algorithm is proposed to address three key aspects: what agents to involve in the communication, what information content to share, and how often to share it. We introduce the notion of a connectivity network, modelled as a weighted graph, where nodes represent agents and edges represent the degree of connectivity between pairs of agents. The optimal graph topology is learned end-to-end concurrently with the stochastic policy so as to maximise future expected returns. The communication patterns depend on the graph's topology through a diffusion process on the graph, the heat kernel, which is found by exponentiating the Laplacian eigen-system through time and is fully differentiable. Empirical results show that CDC is capable of superior performance over alternative algorithms for a range of cooperative navigation tasks.

1. Introduction

In Deep Reinforcement Learning (RL), an agent learns to take sequential decisions by mapping its observations of the world to actions using a reward as feedback signal (Sutton & Barto, 1998). DRL has achieved unprecedented performance in many single-agent problems such as playing the game of Go (Silver et al., 2016), Atari videogames (Mnih et al., 2015; Vinyals et al., 2019), and autonomous robot locomotion (Lillicrap et al., 2015). Recent efforts are being spent on modelling real-world systems characterised by multiple interacting agents that need to cooperatively accomplish a particular goal such as those arising in robot navigation (Tanner & Kumar, 2005), autonomous vehicles coordination (Brunet et al., 1995), traffic management (Dresner & Stone, 2004), supply chain management (Lee & Kim, 2008) and multi-player games (Vinyals et al., 2017). Exten-

sions of single-agent DRL techniques have recently been investigated to enable multi-agent reinforcement learning (MARL). In a multi-agent extension of Deep Deterministic Policy Gradient (DDPG) (Lillicrap et al., 2015), a critic has access to observations and actions from all agents, and provides feedback to each actor (Lowe et al., 2017). The notion of a centralised critic has also been utilised to improve overall coordination in cooperative settings (Foerster et al., 2017), and to implement attention mechanisms (Iqbal & Sha, 2019). A curriculum learning strategy for DDPG, Deep Q-Network (DQN) (Mnih et al., 2013), and Trust Region Policy Optimization (TRPO) (Schulman et al., 2015) has been tested on various cooperative tasks such as pursuit-evasion and coordinating bipedal walkers, and has been shown to scale well with the number of agents (Gupta et al., 2017).

One of the fundamental challenges in cooperative multi-agent domains is the need to provide agents with the ability to develop adequate communication strategies. The fact that communication plays a critical role in achieving synchronization in multi-agent systems has been well documented (Vorobeychik et al., 2017; Demichelis & Weibull, 2008; Miller & Moser, 2004; Kearns, 2012; Foerster et al., 2016; Sukhbaatar et al., 2016; Singh et al., 2019; Pesce & Montana, 2019). In order to determine an effective communication strategy, three key aspects need to be taken into account: what messages need to be exchanged, when to share the messages, and with whom to communicate. The first one of the above three challenges, i.e. what to communicate, has been attacked in a number of different ways. For instance, in Foerster et al. (2016), the information content to be shared amongst agents is propagated through differential channels, allowing the gradient to flow from agent to agent and provide appropriate feedback. In Sukhbaatar et al. (2016), a large neural network receives observations from all agents, and maps local messages received from individual agents onto a global message that is used to generate actions. Bidirectional recurrent neural networks have also been used to connect individual agent policies and Q-Networks, and implement communication mechanisms (Peng et al., 2017). In Pesce & Montana (2019), a memory device is used to implement a shared communication channel, whereby each agent first performs a read operation to extract an informative

¹University of Warwick, Coventry, CV4 7AL, UK. Correspondence to: Giovanni Montana <g.montana@warwick.ac.uk>.

content for itself, and then writes a response message.

Recent DRL methodologies have also been proposed to address the second issue, i.e. when to communicate. For instance, in Jiang & Lu (2018), a learnable attention unit determines whether an agent should communicate with other agents, given its observations and action intentions. In a different approach, a gating mechanism operating on the hidden states of the agents’ neural network policies has been used to decide whether to allow or block messages (Singh et al., 2019). Finally, the problem of dynamically selecting the agents involved in the communication activities has also been investigated. Attention mechanisms have been introduced to enable an agent to determine which interactions contribute the most to the overall performance (Hoshen, 2017) and to explicitly target agents for communication (Das et al., 2018). A learnable scheduler unit has been used to best utilise a shared communication medium with limited bandwidth (Kim et al., 2019). In Wang et al. (2019a) decentralized value functions are found through minimizing the communication between agents, in order to make them individually and communicate only if necessary.

In this paper, we propose a DRL algorithm for cooperative MA scenarios that aims to improve coordination through an learned communication strategy. Our ultimate objective is to address all the three fundamental aspects above - *what*, *when* and *with whom* to communicate - in a unified framework built around a notion of communication networks. The proposed algorithm, Connectivity-driven Communication (CDC), makes use of a time-varying weighted graph whereby each node in the graph represents an agent, and an edge quantifies the degree of connectivity between pairs of agents. The edges of the graphs are learnt by the agents through continuous interactions with the environment, and give rise to time-depending network topologies. The global information flow over the entire network, which depends on the graph’s topology, is then leveraged to define a message-passing strategy. Specifically, we adopt the heat kernel of the graph to dynamically characterise how the information is propagated over the network throughout the learning process. Given a particular graph, the heat kernel simulates a diffusion process of heat transference over time. The heat flow is used by the agents to appropriately weight the messages received by adjacent nodes. During training, the agents discover graph topologies associated to communication patterns able to generate highly rewarded actions. The information to be exchanged amongst agents is also learnt from the observations received by the agents through non-linear mappings.

The proposed CDC algorithm is trained end-to-end, and builds on an extension of the actor-critic paradigm (Degris et al., 2012; Silver et al., 2014; Lillicrap et al., 2015). It is an instance of the Centralized Learning Decentralized execution (CLDE) approach (Foerster et al., 2016; Lowe et al., 2017) whereby additional information is used only

during training, but not during execution. The performance of CDC has been evaluated and compared to other MARL algorithms on four cooperative navigation tasks. Our experimental evidence demonstrates that CDC is capable to outperforming other relevant state-of-the-art algorithms on different performance metrics. In addition, we analyse the communication patterns discovered by the agents in order to illustrate how different topological structures emerge in different scenarios.

2. Connectivity-driven Communication

2.1. Notation and problem setup

We consider Markov Games, a partially observable extension of Markov decision processes (Littman, 1994) involving N interacting agents. We denote by \mathcal{S} the set containing all possible configurations characterising the environment. We use \mathcal{O}_i and \mathcal{A}_i to indicate the sets of all possible observations and actions for the i^{th} agent, $i \in 1, \dots, N$, respectively. Every $\sigma_i^t \in \mathcal{O}_i$ is an agent-specific private representation of the state at time t , and each action $a_i^t \in \mathcal{A}_i$ is deterministically determined by a mapping, $\mu_{\theta_i} : \mathcal{O}_i \mapsto \mathcal{A}_i$, parametrised by θ_i . A transition function $\mathcal{T} : \mathcal{S} \times \mathcal{A}_1 \times \mathcal{A}_2 \times \dots \times \mathcal{A}_N$ describes the behaviour of the environment, and provides the probability to observe a future state, given the current state and all the agents’ actions.

We assume that agents can be modelled as nodes of a communication network that dynamically evolves over time. We introduce a time-varying undirected weighted graph, $G^t = (V, \mathbf{S}^t)$, where V is the set of N nodes, representative of the agents, and $\mathbf{S}^t \in [0, 1]^{V \times V}$ contains the edge weights or connectivity strengths. In our formulation, each $\mathbf{S}^t(u, v) = \mathbf{S}^t(v, u) = s_{u,v}^t$ quantifies the degree of communication between a pair of agents, u and v . Values of $s_{u,v}^t$ that are close to one indicates strong connectivity, and zero values signify no connectivity.

Our rationale is that the agents’ observations at each node can be shared with other agents by propagating the information throughout the graph in a way that takes into account the overall graph topology. As a result of this information propagation process, each agent receives an aggregated message, $\mathbf{m}_u^t \in \mathbb{R}^C$, which is used to determine the agent’s action at time t , i.e.

$$a_u^t = \varphi_{\theta_u^p}(\mathbf{m}_u^t) \quad (1)$$

where $\varphi_{\theta_u^p}$ is a neural network with parameters θ_u^p . The policy of the u^{th} agent, μ_{θ_u} , can be seen as a composition of functions with parameters $\theta_u = \{\theta^g, \theta_u^p\}$, where θ^g is a global set of parameters involved in the communication process, and θ_u^p is used by the u^{th} agent according to Eq. 1. Once each agent has taken an action, the environment generates a reward, $r_i^t : \mathcal{S} \times \mathcal{A}_1 \times \mathcal{A}_2 \times \dots \times \mathcal{A}_N \mapsto \mathbb{R}$. Each agent objective’s is to maximise the discounted sum

of future rewards over time,

$$J(\theta_i) = \mathbb{E}_{a_1^t \sim \mu_1, \dots, a_N^t \sim \mu_N, s^t \sim \mathcal{T}} \left[\sum_{t=0}^T \gamma^t r_i^t(s^t, a_1^t, \dots, a_N^t) \right] \quad (2)$$

where $\gamma \in [0, 1]$ is the discount factor. In our formulation, the connectivity weights are not pre-determined, but are learnt through interactions with the environment in order to identify topological properties yielding efficient communication patterns, and eventually maximizing Eq. 2. This formulation directly addresses the key issue of *when* to communicate, since the graph topology is allowed to vary at each time step, and *who* communicates, since each agent's information is weighted differently over time. In the next section we describe how the time-varying graphs are estimated, and how agents communicate.

2.2. Learning the graph topology

At each time step, upon receiving the private observations, every pair of agents, u and v , exchanges a *local* message,

$$c_{u,v}^t = c_{v,u}^t = \varphi_{\theta^c}(\mathbf{o}_u^t, \mathbf{o}_v^t) \quad (3)$$

where φ_{θ^c} is a neural network with parameter θ^c , and \mathbf{o}_u and \mathbf{o}_v are the observations of u and v , respectively. All such messages exchanged at time t can be arranged in $C^t \in \mathbb{R}^{V \times V \times C}$. The set of local messages received by u is denoted by $\mathbf{c}_u = \cup_{v \in V} c_{v,u}$. Using this information, the connectivity weight between the agents is given by

$$s_{u,v}^t = s_{v,u}^t = \sigma(\varphi_{\theta^s}(\mathbf{c}_{u,v}^t)) \quad (4)$$

where φ_{θ^s} is a neural network with parameter θ^s , and σ is a sigmoid function. Each $s_{u,v}^t$ indicates the strength of the connection between u and v , given the information they share, $\mathbf{c}_{u,v}^t$. All the parameters required for learning the graph topology are included in $\theta^g = \{\theta^s, \theta^c\}$.

2.3. Learning to communicate over graphs

Once that the pair-wise connectivities in Eq. 4 have been determined, and the graph is fully specified, we define a message-passing strategy that takes into account the current network topology. In order to quantify how the information flows over G^t , we make use of the heat kernel, which simulates how energy or heat propagates throughout the network (Kondor & Lafferty, 2002). The heat flow of a graph is governed by its normalised Laplacian (Schoen & Yau, 1994; Chung & Graham, 1997). The Laplacian of G^t is given by $\mathcal{L}^t = D^t - S^t$ where $D^t(u, u) = \sum_{v \in V} s_{u,v}^t$ is the diagonal degree matrix of the graph. The normalised Laplacian is then obtained as: $\hat{\mathcal{L}}^t = \frac{1}{\sqrt{D^t}} \mathcal{L}^t \frac{1}{\sqrt{D^t}}$ which is a fundamental term of the partial differential equation describing the heat diffusion process,

$$\frac{\partial H^t(p)}{\partial p} = -\hat{\mathcal{L}}^t H^t(p). \quad (5)$$

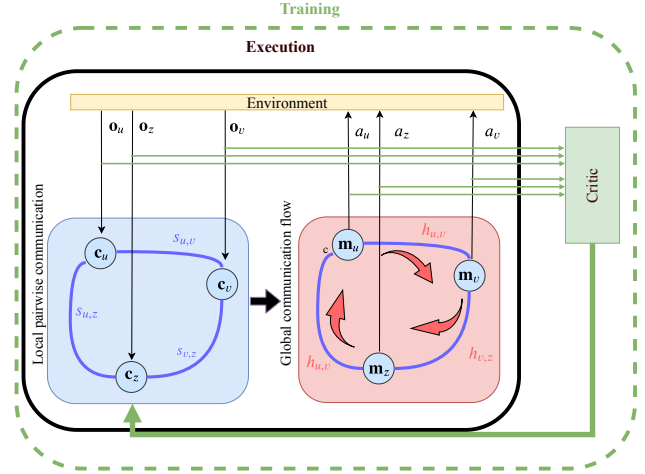


Figure 1: Diagrammatic representation of CDC at a fixed time-step. First, using the agents' observations, local pairwise messages are estimated to generate a communication graph (blue box). Then, the heat kernel is used to quantify the global information flow throughout the graph, and messages are propagated over the graph to generate an aggregated information content at each node (red box), which is mapped on to actions. At training time, observations and actions are utilised by the critic to receive feedback on the graph components.

The heat kernel, $H^t(p) \in \mathbf{R}^{N \times N}$, is the fundamental solution representing the energy flowing through the network at time p . To avoid confusion, the environment time-step is denoted by t , and the time related to the diffusion process is denoted by p . The heat kernel is calculated by using the eigenspectrum formulation of the normalized Laplacian, $\hat{\mathcal{L}}^t = \phi^t \Lambda^t \phi^t$, in which $\Lambda^t = \text{diag}(\lambda_1^t, \dots, \lambda_N^t)$ is a diagonal matrix of eigenvalues ordered by increasing magnitude, and $\phi^t = (\phi_1^t, \dots, \phi_N^t)$ is a matrix with the corresponding eigenvector as columns. For each pair of nodes u and v , the respective heat kernel entry is given by

$$H^t(p)_{u,v} = \phi^t \exp[\Lambda^t p] \phi^{t^T} = \sum_{i=1}^{|V|} \exp[-\lambda_i^t p] \phi_i^t(u) \phi_i^t(v) \quad (6)$$

where $H(p)_{u,v}$ refers to the amount of heat that flowed from u and reached v at time p . This calculation can also be carried out using Padé approximant (Al-Mohy & Higham, 2009), given by $H(p) = \exp[-p \hat{\mathcal{L}}^t]$, which is evaluated over a finite grid of P time points, and for every pair of u and v nodes. Additional details are provided in Section A of Supplementary Material.

For every pair of nodes, we select the time point p_s at which the heat transfer drops by a pre-determined percentage, s , and such that the flow becomes stable afterwards. This results in a matrix, \mathbf{H}^t , whose entries, $\mathbf{H}_{u,v}^t = H_{u,v}^t(p_s)$,

are heat kernel values taken at such times, p_s , i.e.

$$p_s(u, v) = p_{max} : \left| \frac{H^t(p+1)_{u,v} - H^t(p)_{u,v}}{H^t(p)_{u,v}} \right| < s. \quad (7)$$

The CDC algorithm uses these heat kernel values to determine a message-passing mechanism. Specifically, the aggregated information content for agent u is given by

$$\mathbf{m}_u^t = \sum_{v \in V} \mathbf{H}_{u,v}^t \mathbf{c}_{u,v}^t. \quad (8)$$

In this formulation, the overall information content received by agent u is formulated as a linear combination of pair-wise local messages, and is then mapped on to actions through the non-linear mapping defined in Eq. 1. A lack of communication between a pair of agents is imposed when no stable heat kernel value can be found that satisfies Eq. 7.

2.4. Reinforcement learning algorithm

In this section we describe the training algorithm through which all the model parameters are learnt *end-to-end*. We extend the actor-critic framework (Degris et al., 2012), in which an entity called the actor produce actions and another one, the critic, returns feedback on the actor moves. In our formulation, multiple actors, one per every agent, receive feedback from a single centralised critic.

In the standard DDPG (Silver et al., 2014; Lillicrap et al., 2015), the actor $\mu_\theta : \mathcal{O} \mapsto \mathcal{A}$ and the critic $Q^{\mu_\theta} : \mathcal{O} \times \mathcal{A} \mapsto \mathbb{R}$ functions are implemented through neural networks and aim to maximize the expected return $J(\theta) = \mathbb{E}[\sum_{i=1}^T r(\mathbf{o}^t, \mathbf{a}^t)]$. The gradient $\nabla_\theta J(\theta)$ used to update θ is calculated as follows:

$$\nabla_\theta J(\theta) = \mathbb{E}_{\mathbf{o}^t \sim \mathcal{D}} [\nabla_\theta \mu_\theta(\mathbf{o}^t) \nabla_{\mathbf{a}^t} Q^{\mu_\theta}(\mathbf{o}^t, \mathbf{a}^t) |_{\mathbf{a}^t = \mu_\theta(\mathbf{o}^t)}]$$

while Q^{μ_θ} is trained minimizing the following loss:

$$L(\theta) = \mathbb{E}_{\mathbf{o}^t, \mathbf{a}^t, r^t, \mathbf{o}^{t+1} \sim \mathcal{D}} [(Q^{\mu_\theta}(\mathbf{o}^t, \mathbf{a}^t) - y)^2]$$

where $y = r^t + \gamma Q^{\mu'_\theta}(\mathbf{o}^{t+1}, \mathbf{a}^{t+1})$, $Q^{\mu'_\theta}$ is a target critic, whose parameters are only periodically updated with the parameters of Q^{μ_θ} , utilised to stabilize the training.

We follow the CLDE paradigm (Kraemer & Banerjee, 2016; Foerster et al., 2016; Lowe et al., 2017) so that additional information is used during training, but not at execution time. Centralised training can be easily implemented through actor-critic approaches by giving the critics access to global information, whilst restricting the actors to local observations. We adopt a centralised critic that, at training time, uses the observations and actions of all the agents to produce the Q value. In order to make the critic unique for all the agents and to manage to keep the number of parameters constant, we approximate our Q function using a recurrent neural network (RNN). We treat the observa-

tion/action pairs as a sequence with respect to the agents:

$$\mathbf{h}_i^t = \text{RNN}(\mathbf{o}_i^t, \mathbf{a}_i^t | \mathbf{h}_{i-1}^t) \quad (9)$$

where \mathbf{h}_i^t and \mathbf{h}_{i-1}^t are the hidden state produced for the i^{th} and $i-1^{\text{th}}$ agent, respectively. Upon receiving all observation/action pairs from all agents, we use the last hidden state \mathbf{h}_N^t to produce the Q -value:

$$Q(\mathbf{o}_1^t, \dots, \mathbf{o}_N^t, \mathbf{a}_1^t, \dots, \mathbf{a}_N^t) = \varphi_{\theta_Q}(\mathbf{h}_N^t)$$

where φ is a neural network of parameters θ_Q . The parameters of the i^{th} agent are adjusted to maximize the objective function $J(\theta_i) = \mathbb{E}[R_i]$ following the direction of the gradient $J(\theta_i)$:

$$\nabla_{\theta_i} J(\theta_i) = \mathbb{E}_{\mathbf{o}_i^t, \mathbf{a}_i^t, r^t, \mathbf{o}_i^{t+1} \sim \mathcal{D}} [\nabla_{\theta_i} \mu_{\theta_i}(\mathbf{m}_i^t) \nabla_{\mathbf{a}_i^t} Q(\mathbf{x}) |_{\mathbf{a}_i^t = \mu_{\theta_i}(\mathbf{m}_i^t)}]$$

where $\mathbf{x} = (\mathbf{o}_1^t, \dots, \mathbf{o}_N^t, \mathbf{a}_1^t, \dots, \mathbf{a}_N^t)$ and Q minimizes the temporal difference error as follows:

$$L(\theta_i) = \mathbb{E}_{\mathbf{o}_i^t, \mathbf{a}_i^t, r^t, \mathbf{o}_i^{t+1} \sim \mathcal{D}} [(Q(\mathbf{x}) - y)^2]$$

in which:

$$y = r_i^t + \gamma Q(\mathbf{o}_1^{t+1}, \dots, \mathbf{o}_N^{t+1}, \mathbf{a}_1^{t+1}, \dots, \mathbf{a}_N^{t+1})$$

The pseudo-code summarising the proposed learning algorithm is provided in Algorithm 1; see also Figure 4. In the Figure it can be noted that the centralised critic (green) receiving observations and actions to provide feedback to agents is used only during training, and that the graph-driven communication process is also a key component of the proposed model during execution.

3. Experimental results

3.1. Environments

The performance of CDC has been assessed in four different environments. Three of them are commonly used swarm robotic benchmarks - *Navigation Control*, *Formation Control* and *Line Control* (Mesbahi & Egerstedt, 2010; Balch & Arkin, 1998; Agarwal et al., 2019). A fourth one, *Pack Control*, has been added to provide a more challenging task. All the environments have been tested using the Multi-Agent Particle Environment (Lowe et al., 2017; Mordatch & Abbeel, 2017), which allows agents to move around in two-dimensional spaces with discretised action spaces. In *Navigation Control* the agents must move closer to all landmarks whilst avoiding collisions; in *Formation Control* and *Line Control* they must navigate in order to form a polygonal geometric shape centred around the landmark and position themselves along the straight line connecting the two landmarks, respectively; in *Dynamic Pack Control*, worker agents need to follow the leaders to occupy a landmark, that once taken, moves to a different location. Further

	Navigation Control $N = 3$			Navigation Control $N = 10$		
	Reward	# collisions	Distance	Reward	# collisions	Distance
DDPG	-57.3 ± 9.94	1.24 ± 0.39	4.09 ± 6.92	-115.93 ± 21.26	8.83 ± 6.41	3.6 ± 0.85
MADDPG	-45.23 ± 6.59	0.77 ± 0.24	3.16 ± 5.74	-112.17 ± 13.23	12.29 ± 7.45	3.44 ± 0.53
CommNet	-48.95 ± 6.25	0.92 ± 0.24	3.49 ± 5.09	-104.49 ± 10.45	12.21 ± 6.87	3.14 ± 0.41
MAAC	-43.18 ± 6.44	0.71 ± 0.24	1.46 ± 2.97	-107.38 ± 11.81	9.04 ± 6.46	3.26 ± 0.46
ST-MARL	-55.36 ± 8.17	1.54 ± 3.56	1.2 ± 0.33	-110.69 ± 15.75	32.73 ± 32.77	3.27 ± 0.57
CDC	-39.16 ± 4.77	0.56 ± 0.19	0.4 ± 1.66	-102.68 ± 10.1	9.03 ± 9.36	3.06 ± 0.4
	Formation Control $N = 4$			Formation Control $N = 10$		
	Reward	Time	Success Rate	Reward	Time	Success Rate
DDPG	-39.43 ± 12.37	50 ± 0.0	0 ± 0.0	-49.27 ± 6.11	50 ± 0.0	0 ± 0.0
MADDPG	-19.86 ± 6.04	50 ± 0.0	0 ± 0.0	-20.65 ± 7.11	50 ± 0.0	0 ± 0.0
CommNet	-7.77 ± 2.06	45.8 ± 10.19	$0.180.38$	-10.22 ± 1.03	48.89 ± 5.5	0.04 ± 0.2
MAAC	-5.77 ± 1.53	26.66 ± 17.2	0.66 ± 0.47	-9.63 ± 1.35	50 ± 0.0	0 ± 0.0
ST-MARL	-20.24 ± 3.0	50 ± 0.0	0 ± 0.0	-19.81 ± 5.74	50 ± 0.0	0 ± 0.0
CDC	-4.22 ± 1.46	11.82 ± 5.49	0.99 ± 0.12	-7.51 ± 1.06	15.21 ± 9.23	0.99 ± 0.1
	Line Control $N = 4$			Line Control $N = 10$		
	Reward	Time	Success Rate	Reward	Time	Success Rate
DDPG	-33.45 ± 10.58	49.99 ± 0.22	0 ± 0.0	-68.19 ± 10.2	50 ± 0.0	0 ± 0.0
MADDPG	11.55 ± 2.79	47.32 ± 9.14	0.08 ± 0.27	-12.69 ± 2.11	48.48 ± 7.12	0.04 ± 0.21
CommNet	-10.99 ± 2.24	46.97 ± 8.93	0.12 ± 0.33	-9.58 ± 1.28	37.73 ± 14.85	0.47 ± 0.5
MAAC	-7.38 ± 2.09	17.08 ± 12.17	0.89 ± 0.32	-8.58 ± 1.52	22.55 ± 16.09	0.76 ± 0.43
ST-MARL	-23.87 ± 7.77	50 ± 0.0	0 ± 0.0	-19.24 ± 6.26	50 ± 0.0	0 ± 0.0
CDC	-5.97 ± 1.73	10.42 ± 5.58	0.98 ± 0.13	-7.96 ± 1.19	15.06 ± 12.02	0.91 ± 0.29
	Dynamic Pack Control $N = 4$			Dynamic Pack Control $N = 8$		
	Reward	Distance	Targets caught	Reward	Distance	Targets caught
DDPG	-224.77 ± 87.65	3.52 ± 1.67	0 ± 0.0	-279.67 ± 70.18	4.58 ± 1.4	0 ± 0.0
MADDPG	-116.15 ± 71.37	1.46 ± 0.72	0.2 ± 0.13	-110.86 ± 28.66	1.22 ± 0.28	0.0 ± 0.05
CommNet	293.35 ± 446.89	1.11 ± 0.12	0.81 ± 0.89	-76.18 ± 138.73	1.13 ± 0.25	0.07 ± 0.28
MAAC	-95.29 ± 61.65	1.25 ± 0.21	0.01 ± 0.12	-105.15 ± 46.42	1.15 ± 0.28	0.01 ± 0.09
ST-MARL	-107.02 ± 71.84	1.26 ± 0.3	0.02 ± 0.14	-123.91 ± 16.89	1.42 ± 0.36	0 ± 0.0
CDC	369.5 ± 463.92	1.09 ± 0.1	0.96 ± 0.93	58.03 ± 279.05	1.12 ± 0.14	0.35 ± 0.56

Table 1: Comparison of DDPG, MADDPG, CommNet, MAAC, ST-MARL and CDC on all four environments and using two different number of agents in each case. Results are averaged over five different seeds.

details are given in Supplementary Material, Section F.

For each environment we have tested two versions with different number of agents: a *basic* one focusing on solving the designed task when only 3 – 4 agents are involved, and a *scalable* one to show the ability to succeed with a higher number (8 – 10) of agents. The performance of competing MARL algorithms has been assessed using a number of metrics: the *reward*, which quantifies how well a task has been solved (the higher the better); the *distance*, which indicates the amount of navigation carried out by the agents to solve the task (the lower the better); the number of *collisions*, which shows the ability to avoid collisions (the lower the better); the *time* required to solve the task (the lower the better); the *success rate*, defined as the number of times an algorithm has solved a task over the total number of attempts; and *caught targets*, which refers to the number of landmarks that the pack managed to reach. Illustrative videos showing CDC in action on the above environments

can be found online ¹.

3.2. Experimental Setup

For our experiments, we use neural networks with two hidden layers (64 each) to implement the graph generation modules (Eq. 4, 3) and the action selector in Eq. 1. The RNN described in Equation 9 is implemented as a long-short term memory (LSTM) network (Schmidhuber, 1996) with 64 units for the hidden state.

We use the Adam optimizer (Kingma & Ba, 2014) with a learning rate of 10^{-3} for critic and 10^{-4} for policies. Similarly to (Agarwal et al., 2019; Wang et al., 2019b), we set $\theta_1 = \theta_2 = \dots = \theta_N$ in order to make the model invariant to the number of agents. The reward discount factor is set to 0.95, the size of the replay buffer to 10^6 and the batch size to 1,024. At each iteration, we calculate the heat kernel over a finite grid of $P = 300$ time points, with a threshold for getting stable values set to $s = 0.05$. This value has been determined after a study (that we report in Section D

¹<http://bit.ly/37d5Jum>

Algorithm 1 CDC

```

1: Initialize actor  $(\mu_{\theta_1}, \dots, \mu_{\theta_N})$  and critic networks
    $(Q_{\theta_1}, \dots, Q_{\theta_N})$ 
2: Initialize actor target networks  $(\mu'_{\theta_1}, \dots, \mu'_{\theta_N})$  and critic target
   networks  $(Q'_{\theta_1}, \dots, Q'_{\theta_N})$ 
3: Initialize replay buffer  $\mathcal{D}$ 
4: for episode = 1 to  $E$  do
5:   Reset environment,  $\mathbf{o}^1 = \mathbf{o}_1^1, \dots, \mathbf{o}_N^1$ 
6:   for  $t = 1$  to  $T$  do
7:     Generate  $\mathbf{C}^t$  (Eq. 3) and  $\mathbf{S}^t$  (Eq. 4)
8:     for  $p = 1$  to  $P$  do
9:       Compute Heat Kernel  $H(p)^t$  (Eq. 5)
10:    end for
11:    Build  $\mathbf{H}^t$  with stable Heat Kernel values (Eq. 7)
12:    for agent  $i = 1$  to  $N$  do
13:      Produce agent's message  $\mathbf{m}_i^t$  (Eq. 8)
14:      Select action  $a_i^t = \mu_{\theta_i}(\mathbf{m}_i^t)$ 
15:    end for
16:    Execute  $\mathbf{a}^t = (a_1^t, \dots, a_N^t)$ , observe  $r$  and  $\mathbf{o}^{t+1}$ 
17:    Store transaction  $(\mathbf{o}^t, \mathbf{a}^t, r, \mathbf{o}^{t+1})$  in  $\mathcal{D}$ 
18:  end for
19:  for agent  $i = 1$  to  $N$  do
20:    Sample minibatch  $\Theta$  of  $B$  transactions  $(\mathbf{o}, \mathbf{a}, r, \mathbf{o}')$ 
21:    Update critic by minimizing:
22:
23:    
$$L(\theta_i) = \frac{1}{B} \sum_{(\mathbf{o}, \mathbf{a}, r, \mathbf{o}') \in \Theta} (y - Q(\mathbf{o}, \mathbf{a}))^2,$$

24:    where  $y = r_i + \gamma Q(\mathbf{o}', \mathbf{a}')|_{a'_k = \mu'_{\theta_k}(\mathbf{m}'_k)}$ 
25:    in which  $\mathbf{m}'_k$  is global message computed using target
    networks
26:    Update actor according to the policy gradient:
27:    
$$\nabla_{\theta_i} J \approx \frac{1}{B} \sum \left( \nabla_{\theta_i} \mu_{\theta_i}(\mathbf{m}_i) \nabla_{a_i} Q^{\mu_{\theta_i}}(\mathbf{o}, \mathbf{a}) \Big|_{a_i = \mu_{\theta_i}(\mathbf{m}_i)} \right)$$

28:  end for
29:  Update target networks:
30:   $\theta'_i = \tau \theta_i + (1 - \tau) \theta'_i$ 
31: end for

```

of Supplementary material) conducted to determine the best threshold to apply. The number of time steps for episode, T , is set to 50 for all the environments, except for Navigation Control where is set to 25. For Formation Control, Line Control and Pack Control the number E of episodes is set to 50,000 for the basic versions (30,000 for scalable versions), while for Navigation Control is set to 100,000 (30,000 for scalable versions).

All network parameters are updated every time 100 new samples are added to the replay buffer. Soft updates with target networks use $\tau = 0.01$. We adopt the low-variance gradient estimator Gumbel-Softmax for discrete actions in order to allow the back-propagation to work properly with categorical variable, which can truncate the gradient's flow. All the presented results are produced by running every experiment 5 times with different seeds (1,2001,4001,6001,8001) in order to avoid that a particular choice of the seed can significantly condition the final performance. Python 3.6.6 (Van Rossum & Drake Jr, 1995) with PyTorch 0.4.1 (Paszke et al., 2017) is used as framework for machine learning and automatic differentiable computing. NetworkX 2.2 (Hagberg et al.,

2008) has been used for graph analysis. Computations were mainly performed using Intel(R) Xeon(R) CPU E5-2650 v3 at 2.30GHz as CPU and GeForce GTX TITAN X as GPU.

3.3. Main results

We have compared CDC against five different baselines, each one representing a different way to approach the MA coordination problem: independent DDPG (Silver et al., 2014; Lillicrap et al., 2015), MADDPG (Lowe et al., 2017), CommNet (Sukhbaatar et al., 2016), MAAC (Iqbal & Sha, 2019) and ST-MARL (Wang et al., 2019b). Independent DDPG provides the simplest baseline in that each agent works independently to solve the task. MADDPG is a commonly adopted approach whereby each agent has its own critic with access to combined observations and actions from all agents during learning. CommNet implements an explicit form of communication where agents' policies are implemented through a large neural network, in which different agents use different subsets of units. At every time-step each agent's action depends on the local observation and on the average of all other policies hidden states, which are used as messages. MAAC is a state-of-the-art method in which an attention mechanism guides the critics to select the information to be shared with the actors. Table 1 summarises the experimental results obtained from all algorithms across the environments. ST-MARL is a graph-based model designed to capture the spatio-temporal dependency of the seen observations in order to facilitate the agents' cooperation. The metric values are obtained by executing the best model (chosen according to the best average reward returned during training) for an additional 100 episodes. We repeated each experiment using 5 different seeds, and each entry of Table 1 is an average over 500 values.

It can be noted that CDC outperforms the five competitors on all four environments for all the three metrics. For example, on Navigation Control ($N = 3$), the task is solved by minimizing the overall distance travelled and the number of collisions, with an improvement over MAAC algorithm. Better performance is achieved in the scalable version with ten agents. In Formation Control ($N = 4$), the best performance is still achieved by CDC, which was capable to solve the task achieving a success rate close the 1 in the half amount of time of MAAC, while CommNet on this task performs poorly, and DDPG and MADDPG completely fail. In the scalable case, when the level of difficulty is much higher, all the baselines fail to complete the task, while CDC still maintains excellent performance with a success rate of 0.99. In Line Control, both scenarios ($N = 4$ and $N = 10$) are efficiently solved by CDC with higher success rate and in less time than MAAC, while all others drastically fail. For Dynamic Pack Control, amongst the competitors, only CommNet does not fail. This is probably due to the fact that in this environment only the leaders can see the point of interest, hence developing good communicating skills is

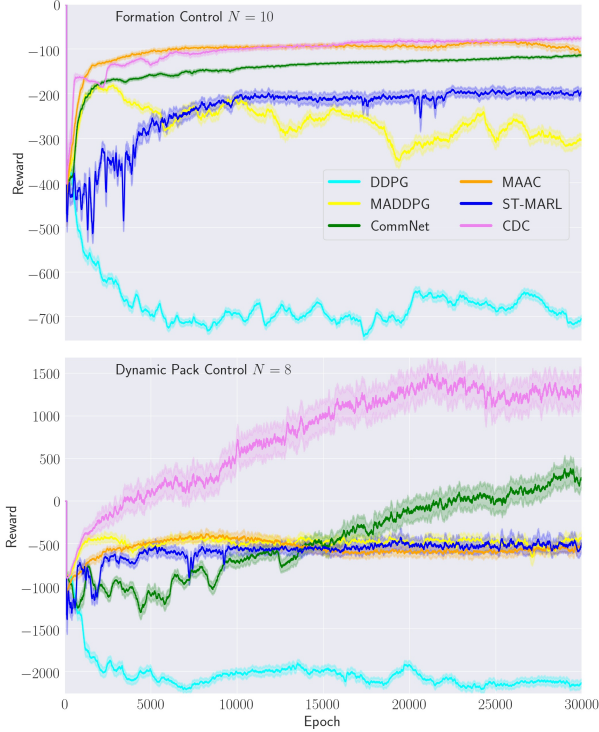


Figure 2: Learning curves for comparison algorithms on Formation Control and Dynamic Pack Control. On the x-axis the number of episodes and on y-axis the achieved rewards. Results are averaged over five different runs.

required to guide the rest of the agents, which otherwise do not know where to go. In this case, CDC also outperforms CommNet on both the number of caught targets and travelled distance. Remarkably, it can be noted that the gains in performance achieved by CDC, compared to other methods, significantly increase when increasing the number of agents. Learning curves for Formation Control and Dynamic Pack Control, averaged over five runs, are shown in Figure 2 (see Supplementary Material Section B.1 for the other environments). Here it can be noticed that CDC reaches the highest reward overall. Of significant interest is the Dynamic Pack Control task for which the only two methods capable to solve it, CommNet and CDC, are those implementing explicit communication mechanisms. With only 4 agents, the reward curves of CommNet, MAAC, and CDC tend to be approximately similar, but increasing the numbers of agents to 8 highlights the remarkable benefits introduced by CDC. We also investigate the performance of CDC when varying the number of agents at execution time (see Supplementary Material, Section E).

3.4. Communication analysis

In this section, we provide an initial qualitative evaluation of the communication patterns that have emerged using CDC on the four environments. Figure 3 shows the communication networks G_H^t as they evolve over time at a given

episode during execution. The black circles represent the landmarks, the blue circles indicate the normal agents, and the red circles the leaders. Their coordinates within the two-dimensional area indicate the navigation trajectories. The lines connecting pairs of agents represent the time-varying edge weights, H^t . Since each $H_{u,v}^t$ quantifies the amount of diffused energy between the two nodes, u and v , Figure 3 illustrates how those quantities evolve over time. Given that these quantities reflect the communication priorities of each agent (Eq. 8), they can be used to interpret which agents are involved in the communication at any given time.

Different patterns emerge in different environments. Figure 3(a) shows that, in the Formation Control environment, the dynamic graphs are highly connected in the early stages of the episodes, and are sparser later on when the formation is found. The degree of topological adjustment observed over time indicate initial bursts of communication activity at the beginning of an episode, while towards the end of it they communicate only with nearby neighbours, which seems to be sufficient to maintain the polygonal shape. A different situation can be observed in the Pack Formation environment, in Figure 3(b). In this case, an intense communication pattern can be observed between leaders and members from an early stage. In fact, the observed topology approximates a bipartite graph between red and blue nodes. This is an expected and plausible pattern, given the nature of this environment. Solving this task requires that the leaders share information with the members, which otherwise would not know the landmark location. Overall, the visualisation of these dynamic graphs learnt by the agents sheds some light on the role players by the diffusion process in facilitating optimal communication mechanism yielding highly rewarding policies. Patterns emerged for the other environments are reported in Section B.2 of the Supplementary Material. In order to further appreciate the role of the heat kernel in driving the communication strategy, Figure 4 provides two different visualisations for two environments (all other environments are reported in Section B.3). On the left, the connection weights are visualised using a circular layout. Here the nodes represent agents, and the size of each node is proportional to the node’s eigenvector centrality. The eigenvector centrality is a popular graph spectral measure (Bonacich, 2007), utilised to determine the influence of a node considering both its adjacent connections and the importance of its neighbouring node. This measure is calculated using the stable heat diffused values averaged over an episode, i.e. $H_{u,v} = (\sum_{t=1}^T H_{u,v}^t)/T$. The resulting graph structure reflects the overall communication patterns emerged while solving the given tasks. On the right, we visualise the squared $N \times N$ matrix of averaged pairwise diffusion values as a heatmap (red values are higher). It can be noted that, in the Pack Control environment, two main communities of agents are formed, each one with a leader. Here, as expected, leaders appear to be very influential nodes

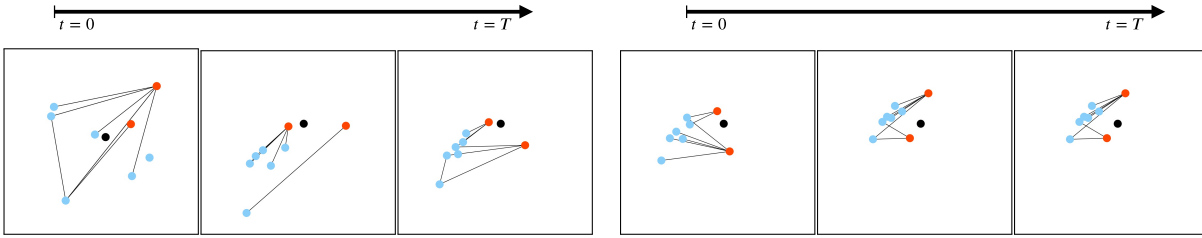


Figure 3: Illustrations of communication networks G_H^t evolving over different episode time-steps Formation Control and Dynamic Pack Control. Black circles represent landmarks; agents are represented in blue; in (b) red circles leader agents are indicated in red. Connections represent the stable heat kernel values utilised in the communication process.

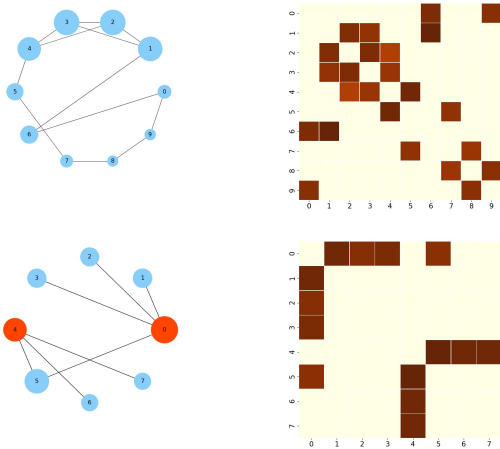


Figure 4: Averaged communication graphs for Formation Control (line above) and Pack Control (line below). On the left, node sizes indicate the eigenvector centrality, connections the stable heat kernel values, while numbers the node labels. On the right, diffused values are shown as heatmaps, where axis numbers correspond to node labels.

(red nodes), and the heatmap shows that the connections between individual members and leaders are very strong. A different pattern emerges instead in Formation Control, where there is no evidence of communities since all nodes are connected to nearly form a circular shape. The corresponding heatmap shows the heat kernel values connecting neighbouring agents tend to assume higher values compared to more distant agents.

4. Conclusions

In this work, we have presented a novel approach to multi-agent reinforcement learning that uses the topology of a time-varying communication network to facilitate communication and cooperation. Unlike other approaches using networks to model multi-agent systems, our CDC algorithm learns the optimal time-evolving graph topology concurrently to the agents’ policy through trial and error in order to maximise future expected results. The agents are equipped

with a mechanism to learn what messages should be shared with others, how often, and with whom, using diffusion processes on graphs. Specifically, we have used the heat kernel as a tool for quantitatively assessing how the information propagates through the communication network. The heat kernel has previously been used in many applications involving graph-valued data (Chung et al., 2016a; Kloster & Gleich, 2014; Xie et al., 2015), but not as a message-passing device to facilitate communication in multi-agent RL settings. Our experimental results on four different environments have demonstrated that, compared to other baselines, CDC can achieve superior performance on navigation tasks of increasing complexity, and remarkably so when the number of agents increases.

Graph-theoretical approaches have previously appeared in multi-agent RL domains, albeit in different ways. For example, Sparse Cooperative Q-Learning (Kok & Vlassis, 2006) is a model-free reinforcement learning algorithm in which the approximation of the global action-state function is based on a coordination graph (Guestrin et al., 2002). Kuyer et al. (2008) proposed a model based on coordination graphs and max-plus algorithm (Kschischang et al., 2001) in order to optimize the behaviour of traffic lights with the aim of reducing congestions. In a more recent approach (Agarwal et al., 2019), a graph is proposed to model not only agents, but also other entities present in the environment, and establish a communication amongst all of them. The intra-agent communication is based on an attention mechanism that weights the messages coming from the adjacent connections of each agent. While this work uses well defined graph structures, the communication process does not exploit the intrinsic properties of the networks. Instead, agents’ actions are taken on the ground of the information coming from their neighbours aggregated through an attention mechanism.

In the near future, we aim to further investigate alternative fully-differentiable mechanisms for message propagation over networks that can be learned during training concurrently with the policy and yield improved communication patterns, e.g. different diffusion models. In addition, we intend to conduct more experiments to extend the analyses

presented in the Supplementary Material (Sec E), and further explore how the learnt graph topologies can facilitate the learning process in scenarios where the number of agents is changing at run-time.

References

- Agarwal, A., Kumar, S., and Sycara, K. Learning transferable cooperative behavior in multi-agent teams. *arXiv preprint arXiv:1906.01202*, 2019.
- Al-Mohy, A. H. and Higham, N. J. A new scaling and squaring algorithm for the matrix exponential. *SIAM Journal on Matrix Analysis and Applications*, 31(3):970–989, 2009.
- Balch, T. and Arkin, R. C. Behavior-based formation control for multirobot teams. *IEEE transactions on robotics and automation*, 14(6):926–939, 1998.
- Bonacich, P. Some unique properties of eigenvector centrality. *Social networks*, 29(4):555–564, 2007.
- Brunet, C.-A., Gonzalez-Rubio, R., and Tetreault, M. A multi-agent architecture for a driver model for autonomous road vehicles. In *Proceedings 1995 Canadian Conference on Electrical and Computer Engineering*, volume 2, pp. 772–775. IEEE, 1995.
- Cheng, A. H.-D. and Cheng, D. T. Heritage and early history of the boundary element method. *Engineering Analysis with Boundary Elements*, 29(3):268–302, 2005.
- Chung, A. W., Pesce, E., Monti, R. P., and Montana, G. Classifying hcp task-fMRI networks using heat kernels. In *2016 International Workshop on Pattern Recognition in NeuroImaging (PRNI)*, pp. 1–4. IEEE, 2016a.
- Chung, A. W., Schirmer, M., Krishnan, M. L., Ball, G., Aljabar, P., Edwards, A. D., and Montana, G. Characterising brain network topologies: a dynamic analysis approach using heat kernels. *Neuroimage*, 141:490–501, 2016b.
- Chung, F. R. and Graham, F. C. *Spectral graph theory*. Number 92. American Mathematical Soc., 1997.
- Das, A., Gervet, T., Romoff, J., Batra, D., Parikh, D., Rabat, M., and Pineau, J. Tarmac: Targeted multi-agent communication. *arXiv preprint arXiv:1810.11187*, 2018.
- Degrís, T., White, M., and Sutton, R. S. Off-policy actor-critic. *arXiv preprint arXiv:1205.4839*, 2012.
- Demichelis, S. and Weibull, J. W. Language, meaning, and games: A model of communication, coordination, and evolution. *American Economic Review*, 98(4):1292–1311, 2008.
- Dresner, K. and Stone, P. Multiagent traffic management: A reservation-based intersection control mechanism. In *Proceedings of the Third International Joint Conference on Autonomous Agents and Multiagent Systems-Volume 2*, pp. 530–537. IEEE Computer Society, 2004.
- Foerster, J., Assael, I. A., de Freitas, N., and Whiteson, S. Learning to communicate with deep multi-agent reinforcement learning. In *Advances in Neural Information Processing Systems*, pp. 2137–2145, 2016.
- Foerster, J., Farquhar, G., Afouras, T., Nardelli, N., and Whiteson, S. Counterfactual multi-agent policy gradients. *arXiv preprint arXiv:1705.08926*, 2017.
- Guestrin, C., Koller, D., and Parr, R. Multiagent planning with factored mdps. In *Advances in neural information processing systems*, pp. 1523–1530, 2002.
- Gupta, J. K., Egorov, M., and Kochenderfer, M. Cooperative multi-agent control using deep reinforcement learning. In *International Conference on Autonomous Agents and Multiagent Systems*, pp. 66–83. Springer, 2017.
- Hagberg, A., Swart, P., and S Chult, D. Exploring network structure, dynamics, and function using networkx. Technical report, Los Alamos National Lab.(LANL), Los Alamos, NM (United States), 2008.
- Hoshen, Y. Vain: Attentional multi-agent predictive modeling. In *Advances in Neural Information Processing Systems*, pp. 2701–2711, 2017.
- Iqbal, S. and Sha, F. Actor-attention-critic for multi-agent reinforcement learning. *ICML*, 2019.
- Jiang, J. and Lu, Z. Learning attentional communication for multi-agent cooperation. *arXiv preprint arXiv:1805.07733*, 2018.
- Kearns, M. Experiments in social computation. *Communications of the ACM*, 55(10):56–67, 2012.
- Kim, D., Moon, S., Hostallero, D., Kang, W. J., Lee, T., Son, K., and Yi, Y. Learning to schedule communication in multi-agent reinforcement learning. *arXiv preprint arXiv:1902.01554*, 2019.
- Kingma, D. P. and Ba, J. Adam: A method for stochastic optimization. *arXiv preprint arXiv:1412.6980*, 2014.
- Kloster, K. and Gleich, D. F. Heat kernel based community detection. In *Proceedings of the 20th ACM SIGKDD international conference on Knowledge discovery and data mining*, pp. 1386–1395. ACM, 2014.
- Kok, J. R. and Vlassis, N. Collaborative multiagent reinforcement learning by payoff propagation. *Journal of Machine Learning Research*, 7(Sep):1789–1828, 2006.

- Kondor, R. and Lafferty, J. Diffusion kernels on graphs and other discrete input spaces. *icml 2002*. In *Proc*, pp. 315–322, 2002.
- Kraemer, L. and Banerjee, B. Multi-agent reinforcement learning as a rehearsal for decentralized planning. *Neuro-computing*, 190:82–94, 2016.
- Kschischang, F. R., Frey, B. J., Loeliger, H.-A., et al. Factor graphs and the sum-product algorithm. *IEEE Transactions on information theory*, 47(2):498–519, 2001.
- Kuyer, L., Whiteson, S., Bakker, B., and Vlassis, N. Multi-agent reinforcement learning for urban traffic control using coordination graphs. In *Joint European Conference on Machine Learning and Knowledge Discovery in Databases*, pp. 656–671. Springer, 2008.
- Lee, J.-H. and Kim, C.-O. Multi-agent systems applications in manufacturing systems and supply chain management: a review paper. *International Journal of Production Research*, 46(1):233–265, 2008.
- Lillicrap, T. P., Hunt, J. J., Pritzel, A., Heess, N., Erez, T., Tassa, Y., Silver, D., and Wierstra, D. Continuous control with deep reinforcement learning. *CoRR*, abs/1509.02971, 2015.
- Littman, M. L. Markov games as a framework for multi-agent reinforcement learning. In *Machine Learning Proceedings 1994*, pp. 157–163. Elsevier, 1994.
- Lowe, R., Wu, Y., Tamar, A., Harb, J., Abbeel, O. P., and Mordatch, I. Multi-agent actor-critic for mixed cooperative-competitive environments. In *Advances in Neural Information Processing Systems*, pp. 6379–6390, 2017.
- Mesbahi, M. and Egerstedt, M. *Graph theoretic methods in multiagent networks*, volume 33. Princeton University Press, 2010.
- Miller, J. H. and Moser, S. Communication and coordination. *Complexity*, 9(5):31–40, 2004.
- Mnih, V., Kavukcuoglu, K., Silver, D., Graves, A., Antonoglou, I., Wierstra, D., and Riedmiller, M. Playing atari with deep reinforcement learning. *arXiv preprint arXiv:1312.5602*, 2013.
- Mnih, V., Kavukcuoglu, K., Silver, D., Rusu, A. A., Veness, J., Bellemare, M. G., Graves, A., Riedmiller, M., Fidjeland, A. K., Ostrovski, G., et al. Human-level control through deep reinforcement learning. *Nature*, 518(7540): 529, 2015.
- Mordatch, I. and Abbeel, P. Emergence of grounded compositional language in multi-agent populations. *arXiv preprint arXiv:1703.04908*, 2017.
- Paszke, A., Gross, S., Chintala, S., Chanan, G., Yang, E., DeVito, Z., Lin, Z., Desmaison, A., Antiga, L., and Lerer, A. Automatic differentiation in pytorch, 2017.
- Peng, P., Yuan, Q., Wen, Y., Yang, Y., Tang, Z., Long, H., and Wang, J. Multiagent bidirectionally-coordinated nets for learning to play starcraft combat games. *arXiv preprint arXiv:1703.10069*, 2017.
- Pesce, E. and Montana, G. Improving coordination in multi-agent deep reinforcement learning through memory-driven communication. *Deep Reinforcement Learning Workshop, (NeurIPS 2018), Montreal, Canada*, 2019.
- Schmidhuber, J. A general method for multi-agent reinforcement learning in unrestricted environments. In *Adaptation, Coevolution and Learning in Multiagent Systems: Papers from the 1996 AAAI Spring Symposium*, pp. 84–87, 1996.
- Schoen, R. and Shing-Tung Yau Mack, C. A. *Lectures on Differential Geometry*. International Press, 1994.
- Schoen, R. and Yau, S.-T. *Lectures on differential geometry*, volume 2. International press Cambridge, MA, 1994.
- Schulman, J., Levine, S., Abbeel, P., Jordan, M., and Moritz, P. Trust region policy optimization. In *International conference on machine learning*, pp. 1889–1897, 2015.
- Silver, D., Lever, G., Heess, N., Degris, T., Wierstra, D., and Riedmiller, M. Deterministic policy gradient algorithms. In *ICML*, 2014.
- Silver, D., Huang, A., Maddison, C. J., Guez, A., Sifre, L., Van Den Driessche, G., Schrittwieser, J., Antonoglou, I., Panneershelvam, V., Lanctot, M., et al. Mastering the game of go with deep neural networks and tree search. *nature*, 529(7587):484, 2016.
- Singh, A., Jain, T., and Sukhbaatar, S. Learning when to communicate at scale in multiagent cooperative and competitive tasks. *ICLR*, 2019.
- Sukhbaatar, S., Fergus, R., et al. Learning multiagent communication with backpropagation. In *Advances in Neural Information Processing Systems*, pp. 2244–2252, 2016.
- Sutton, R. S. and Barto, A. G. *Introduction to reinforcement learning*, volume 135. MIT press Cambridge, 1998.
- Tanner, H. G. and Kumar, A. Towards decentralization of multi-robot navigation functions. In *Proceedings of the 2005 IEEE International Conference on Robotics and Automation*, pp. 4132–4137. IEEE, 2005.
- Van Rossum, G. and Drake Jr, F. L. *Python tutorial*. Centrum voor Wiskunde en Informatica Amsterdam, The Netherlands, 1995.

- Vinyals, O., Ewalds, T., Bartunov, S., Georgiev, P., Vezhn-
evets, A. S., Yeo, M., Makhzani, A., Küttler, H., Agapiou,
J., Schrittwieser, J., et al. Starcraft ii: A new challenge for
reinforcement learning. *arXiv preprint arXiv:1708.04782*,
2017.
- Vinyals, O., Babuschkin, I., Czarnecki, W. M., Mathieu, M.,
Dudzik, A., Chung, J., Choi, D. H., Powell, R., Ewalds,
T., Georgiev, P., et al. Grandmaster level in starcraft ii
using multi-agent reinforcement learning. *Nature*, pp.
1–5, 2019.
- Vorobeychik, Y., Joveski, Z., and Yu, S. Does communica-
tion help people coordinate? *PloS one*, 12(2):e0170780,
2017.
- Wang, T., Wang, J., Zheng, C., and Zhang, C. Learning
nearly decomposable value functions via communication
minimization. *arXiv preprint arXiv:1910.05366*, 2019a.
- Wang, Y., Xu, T., Niu, X., Tan, C., Chen, E., and Xiong,
H. Stmarl: A spatio-temporal multi-agent reinforcement
learning approach for traffic light control. *arXiv preprint
arXiv:1908.10577*, 2019b.
- Xiao, B., Wilson, R. C., and Hancock, E. R. Characterising
graphs using the heat kernel. 2005.
- Xie, J., Fang, Y., Zhu, F., and Wong, E. Deepshape: Deep
learned shape descriptor for 3d shape matching and re-
trieval. In *Proceedings of the IEEE Conference on Com-
puter Vision and Pattern Recognition*, pp. 1275–1283,
2015.

Supplementary material

A. Heat kernel: additional details

The heat kernel is a technique from spectral geometry (Schoen & Shing-Tung Yau Mack, 1994), and is a fundamental solution of the *heat equation*:

$$\frac{\partial H^t(p)}{\partial p} = -\hat{\mathcal{L}}^t H^t(p). \quad (10)$$

Given a graph G defined on n vertices, the normalized Laplacian $\hat{\mathcal{L}}$, acting on functions with Neumann boundary conditions (Cheng & Cheng, 2005), is associated with the rate of heat dissipation. $\hat{\mathcal{L}}$ can be written as:

$$\hat{\mathcal{L}} = \sum_{i=0}^{n-1} \lambda_i I_i$$

where I_i is the projection onto the i^{th} eigenfunction ϕ_i . For a given time $t \geq 0$, the heat kernel $H(t)$ is defined as a $n \times n$ matrix:

$$H(t) = \sum_i \exp[-\lambda_i t] I_i = \exp[-t \hat{\mathcal{L}}]. \quad (11)$$

Eq. 11 represents an analytical solution to Eq. 10.

Lemma 1 (Chung & Graham, 1997) *The heat kernel $H(t)$ for a graph G with eigenfunctions θ_i satisfies:*

$$H(t)_{u,v} = \sum_{i=1} \exp[-\lambda_i t] \phi_i(u) \phi_i(v)$$

The proof follows from the fact that

$$H(t) = \sum_i \exp[-\lambda_i t] I_i$$

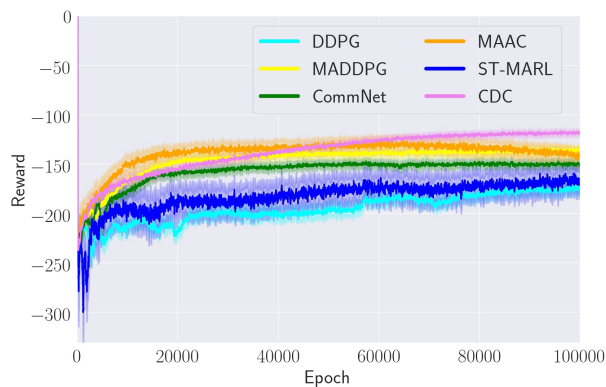
and

$$I(u, v) = \phi_i(u) \phi_i(v).$$

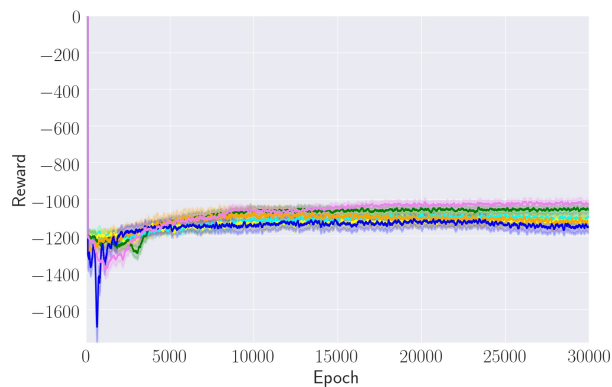
Lemma 1 is provided to explain Eq. 6.

B. Additional results

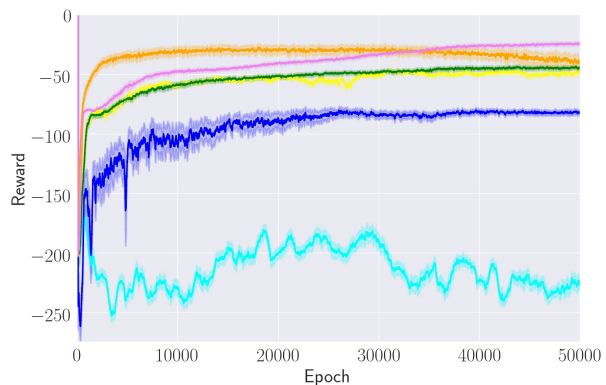
B.1. Learning curves



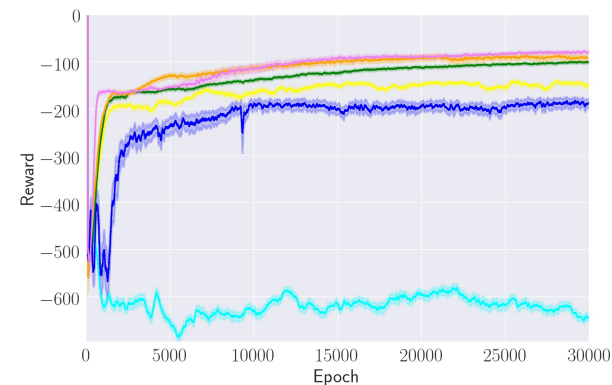
Navigation Control $N = 3$



Navigation Control $N = 10$

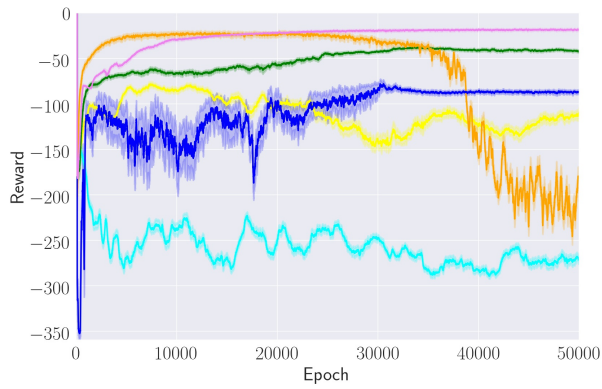


Line Control $N = 4$

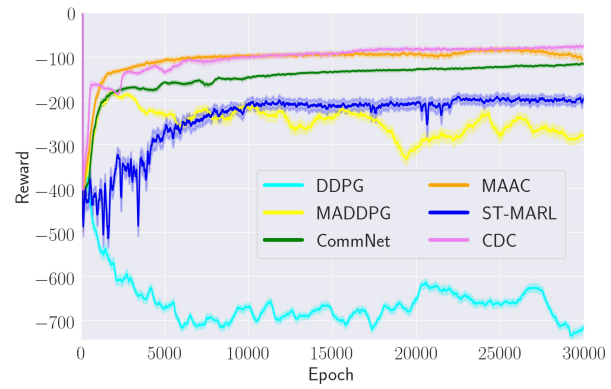


Line Control $N = 10$

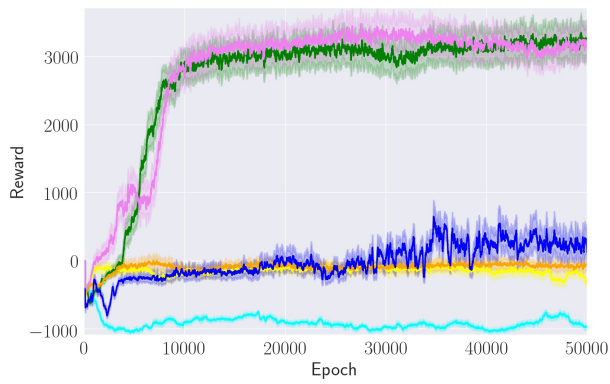
Figure 5: Learning curves for 6 competing algorithms assessed on Navigation Control and Line Control. Horizontal axes report the number of episodes, while vertical axes the achieved rewards. Results are averaged over five different runs.



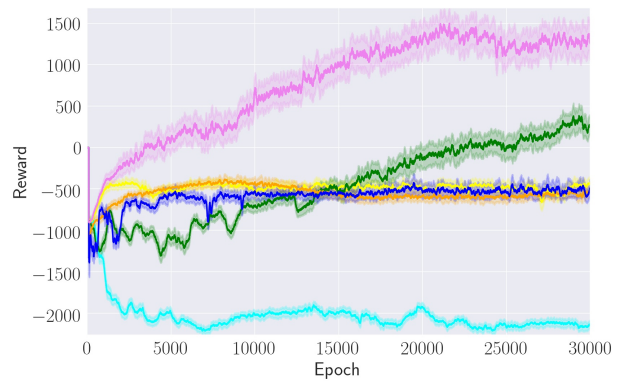
Formation Control $N = 4$



Formation Control $N = 10$



Dynamic Pack Control $N = 4$



Dynamic Pack Control $N = 10$

Figure 6: Learning curves for comparison algorithms on Formation Control and Dynamic Pack Control. Horizontal axes report the number of episodes, while vertical axes the achieved rewards. Results are averaged over five different runs.

B.2. Communication networks

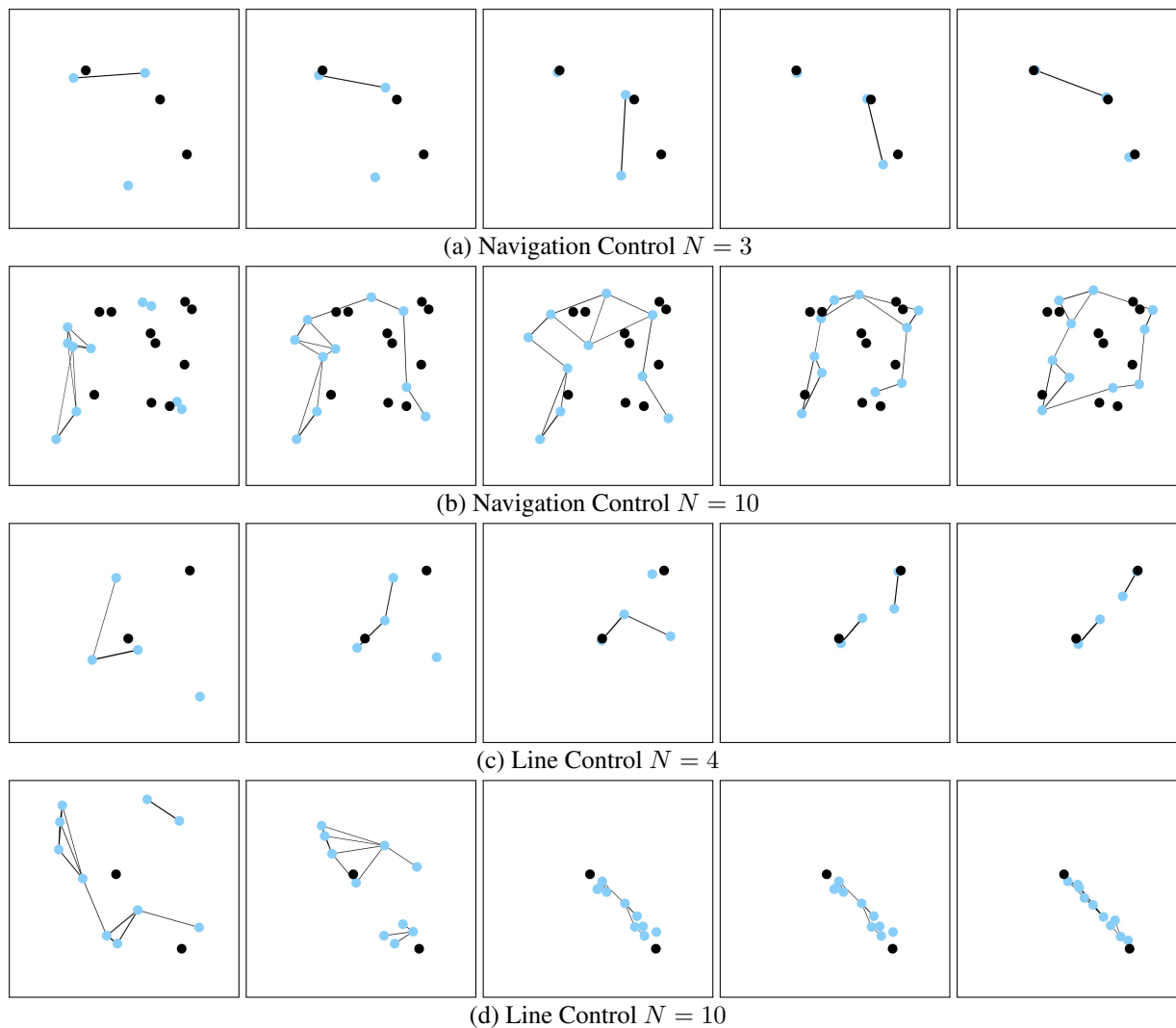


Figure 7: Illustrations of communication networks G_H^t evolving over different episode time-steps.

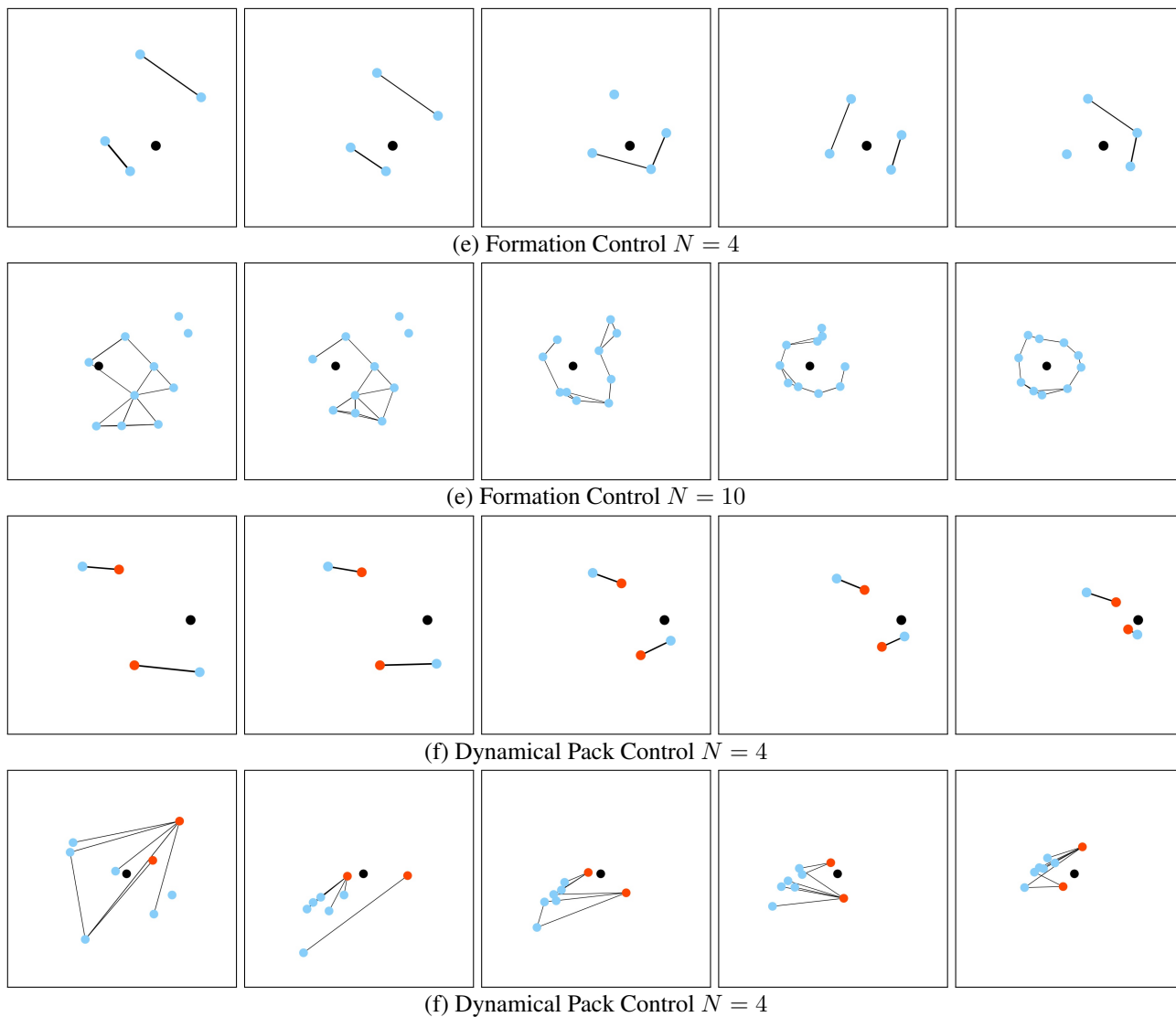


Figure 8: Illustrations of communication networks G_H^t evolving over different episode time-steps.

B.3. Average communication graphs

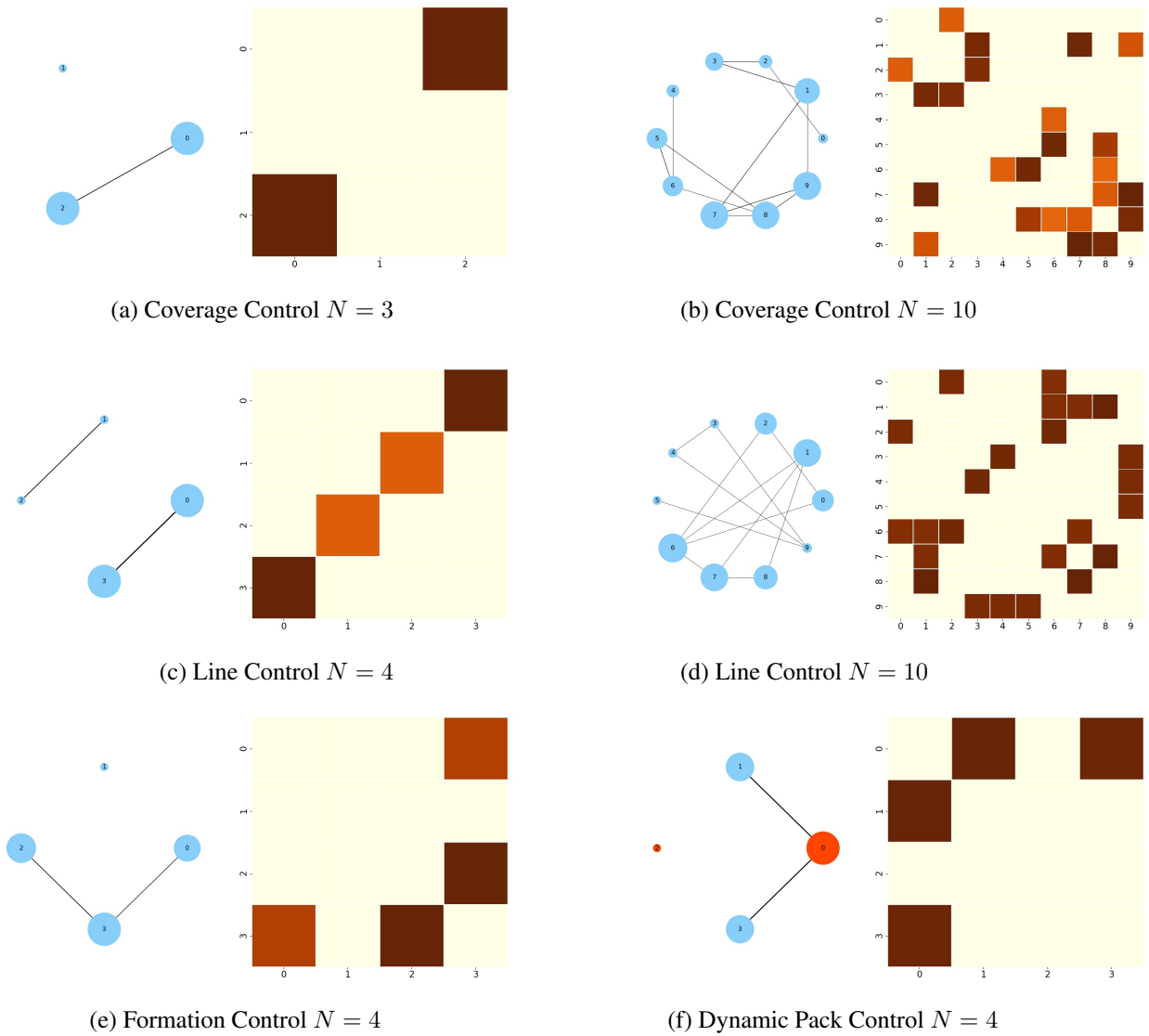


Figure 9: Communication graphs averaged over an episode. For each environment, on the left, node sizes indicate the eigenvector centrality, connections the stable heat kernel values, while numbers the node labels. Here, a circular layout is used to represent the graphs in order to provide an alternative view where connection patterns can result easier to detect. On the right, diffused values are shown as heatmaps, where axis numbers correspond to node labels.

C. Ablation study

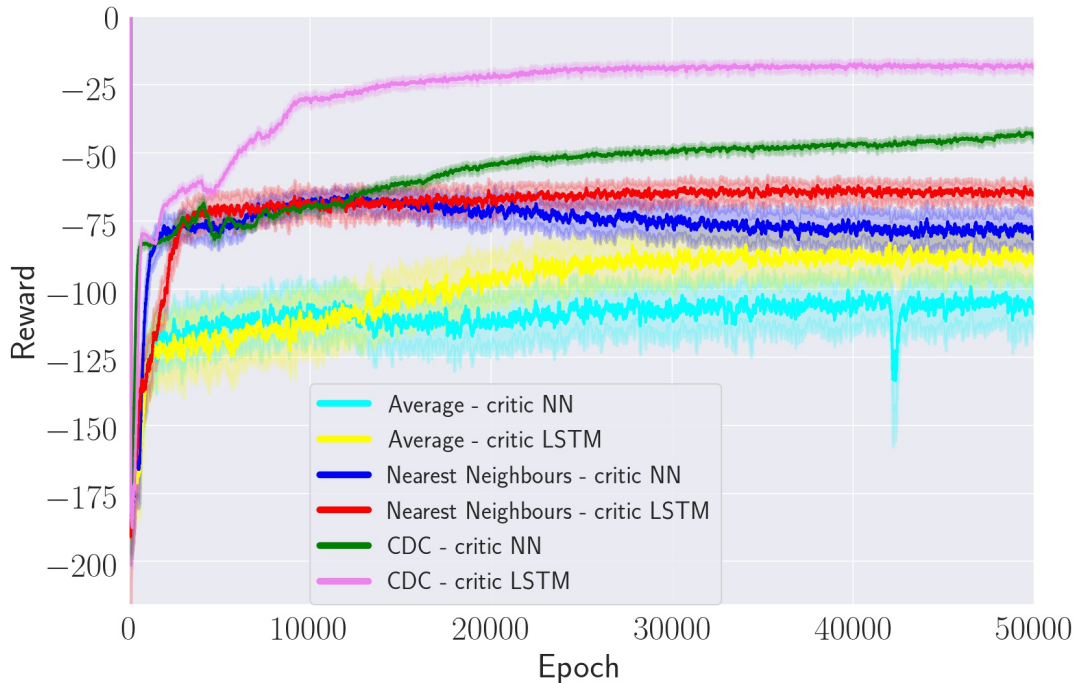


Figure 10: Learning curves of different versions of the proposed model on Formation Control ($N = 4$).

In this section we present the results of an ablation study that has been carried out to investigate the specific benefits of the heat kernel over alternative and simpler information propagation mechanisms. In the *average* version, every agent takes an action after receiving an average of the observations of all other agents, whereas in the *nearest neighbours* version only the observations of an agent’s two nearest neighbours are averaged. For each one of these two mechanisms, we compare a version using the adopted critic (Section 2.4), which uses an RNN (specifically an LSTM), and the version using the traditional critic, which is based on a feed-forward neural network (NN).

In Figure 10, it can be noted that the heat kernel achieves the highest performance. Both versions of CDC, with LSTM and without, outperform the others. The results also show that the nearest neighbours version reaches better outcomes compared to the average version; this suggests that averaging all observations lead to noisier embeddings, and limits the effectiveness of the method. Overall, we have observed that using the LSTM-based critic leads to better performance overall. This result is somewhat expected given that the LSTM is able to filter out irrelevant information from a sequence of observations, and can retain only relevant information in its hidden state.

D. Choosing the heat kernel threshold

Method	Formation Control $N = 4$		
	Reward	Time	Success Rate
CDC $s = 0.01$	$-4.48 \pm (1.62)$	$13.52 \pm (9.83)$	$0.93 \pm (0.21)$
CDC $s = 0.025$	$-4.33 \pm (1.28)$	$14.01 \pm (9.74)$	$0.94 \pm (0.24)$
CDC $s = 0.05$	$-4.22 \pm (1.46)$	$11.82 \pm (5.49)$	$0.99 \pm (0.1)$
CDC $s = 0.075$	$-4.34 \pm (1.43)$	$12.88 \pm (9.13)$	$0.95 \pm (0.22)$
CDC $s = 0.1$	$-4.31 \pm (1.57)$	$12.52 \pm (8.39)$	$0.96 \pm (0.2)$

Table 2: Comparison of CDC results using different values for threshold s

Table 2 reports on the performance of CDC on Formation Control when the threshold parameter s varies over a grid of possible values (see Eq. 7). In turn, this threshold determines whether the heat kernel values are stable or not. The best performance is obtained using $s = 0.05$, which is the value used in all our experiments. To select the thresholds to test in Table 2, we defined a range of values close to solutions which have been proven to be successful in other heat kernel related works (Chung et al., 2016b; Xiao et al., 2005).

E. Varying the number of agents

# agents	DDPG	CDC
3	2.34 ± 0.61	1.06 ± 0.12
4	3.52 ± 1.67	1.09 ± 0.1
5	3.90 ± 1.68	1.08 ± 0.15
6	4.44 ± 1.7	1.08 ± 0.18
7	5.21 ± 1.98	1.12 ± 0.12
8	6.49 ± 2.17	1.13 ± 0.11

Table 3: Comparison of DDPG and CDC on Dynamic Pack Control. Both algorithms were trained with 4 agents and tested with 3-8. The performance metric used here is the distance of the the farthest agent to the landmark.

We tested whether CDC is capable of handling a different number of agents at test time. Table 3 shows how the performance of DDPG and CDC compares when they are both trained using 4 learners, but 3-8 agents are used at test time. We report on the maximum distance between the farthest agent and the landmark, which is invariant to the number of agents. It can be noted that CDC can handle systems with a varying number of agents, outperforming DDPG and keeping the final performance competitive with other methods that have been trained with a larger number of agents (see Table 1).

F. Environment details

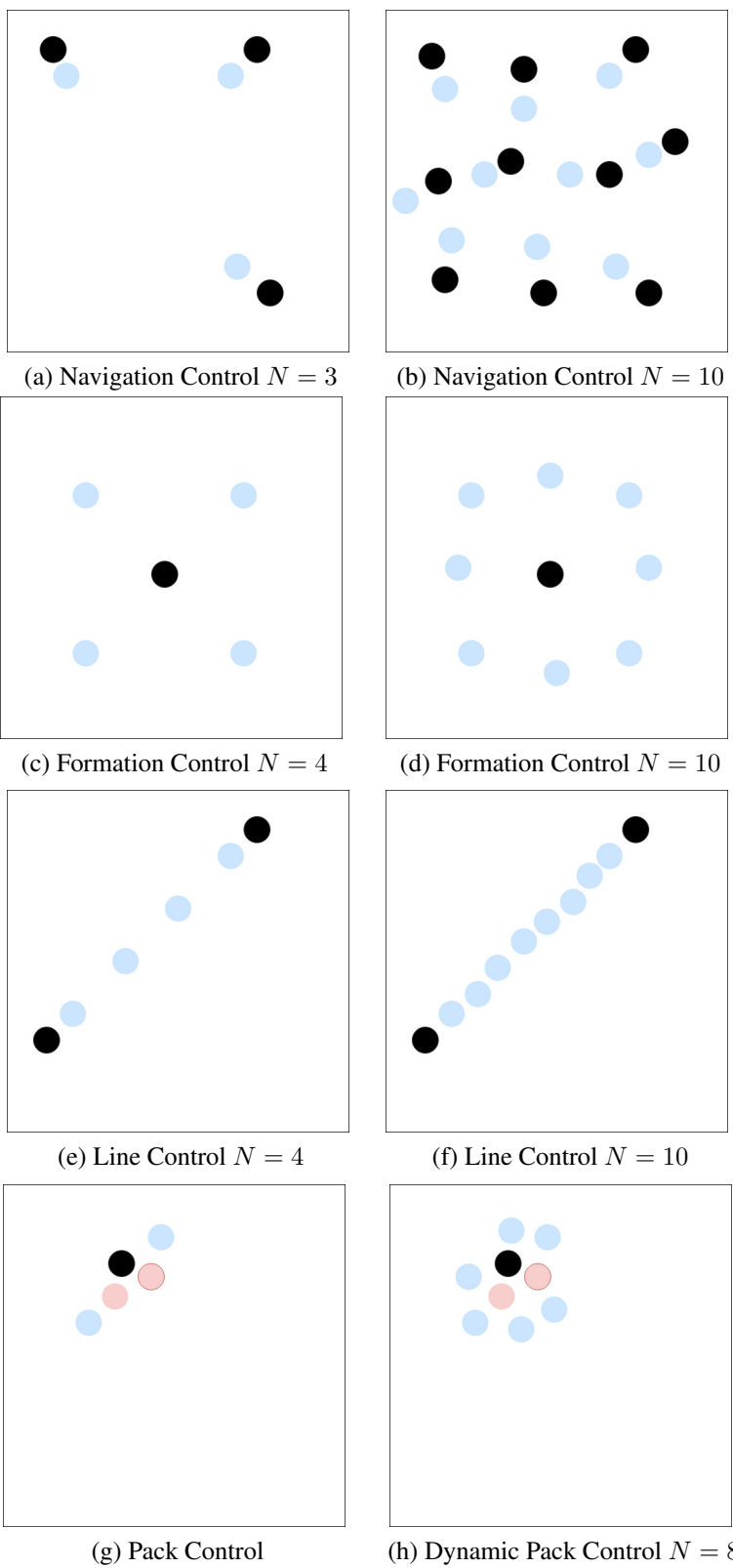


Figure 11: Representations of all the utilised environments.

Navigation Control. There are N agents and N fixed landmarks. The agents must move closer to all landmarks whilst avoiding collisions. Landmarks are not assigned to particular agents, and the agents are rewarded for minimizing the distances between their positions and the landmarks' positions. Each agent can observe the position of all the landmarks and other agents.

Formation Control. There are N agents and only one landmark. In this scenario, the agents must navigate in order to form a polygonal geometric shape, whose shape is defined by the N agents, and centred around the landmark. The agents' objective is to minimize the distances between their locations and the positions required to form the expected shape. Each agent can observe the landmark only.

Line Control. There are N agents and two landmarks. The agents must navigate in order to position themselves along the straight line connecting the two landmarks. Similarly to Formation Control, the agents objective is to minimize the distances between their locations and the positions required to form the expected shape. Each agent can observe the landmarks only.

Dynamic Pack Control. There are N agents, of which two are leaders and $N - 2$ are members, and one landmark. The objective of this task is to simulate a pack behaviour, where agents have to navigate to reach the landmark. Once a landmark is occupied, it moves to a different location. The landmark location is accessible only to the leaders, while the members are blind, i.e. they can only see their current location.